Hindawi Publishing Corporation
Mathematical Problems in Engineering
Volume 2015, Article ID 396305, 12 pages
http://dx.doi.org/10.1155/2015/396305

Research Article

Takagi-Sugeno Fuzzy Model of a One-Half Semiactive Vehicle Suspension: Lateral Approach

L. C. Félix-Herrán,[1] D. Mehdi,[2] J. J. Rodríguez-Ortiz,[3] R. Ramírez-Mendoza,[3] and R. Soto[3]

[1]*Escuela de Ingeniería y Ciencias, Tecnológico de Monterrey, Boulevard Enrique Mazón López 965, 63000 Hermosillo, SON, Mexico*
[2]*LIAS-ENSIP, Université de Poitiers, Bâtiment B25, 2 rue Pierre Brousse, 86022 Poitiers Cedex, France*
[3]*Escuela de Ingeniería y Ciencias, Tecnológico de Monterrey, Avenida Eugenio Garza Sada 2501 Sur, 64849 Monterrey, NL, Mexico*

Correspondence should be addressed to L. C. Félix-Herrán; lcfelix@itesm.mx

Received 16 March 2015; Accepted 3 June 2015

Academic Editor: Qingling Zhang

Copyright © 2015 L. C. Félix-Herrán et al. This is an open access article distributed under the Creative Commons Attribution License, which permits unrestricted use, distribution, and reproduction in any medium, provided the original work is properly cited.

This work presents a novel semiactive model of a one-half lateral vehicle suspension. The contribution of this research is the inclusion of actuator dynamics (two magnetorheological nonlinear dampers) in the modelling, which means that more realistic outcomes will be obtained, because, in real life, actuators have physical limitations. Takagi-Sugeno (T-S) fuzzy approach is applied to a four-degree-of-freedom (4-DOF) lateral one-half vehicle suspension. The system has two magnetorheological (MR) dampers, whose numerical values come from a real characterization. T-S allows handling suspension's components and actuator's nonlinearities (hysteresis, saturation, and viscoplasticity) by means of a set of linear subsystems interconnected via fuzzy membership functions. Due to their linearity, each subsystem can be handled with the very well-known control theory, for example, stability and performance indexes (this is an advantage of the T-S approach). To the best of authors' knowledge, reported work does not include the aforementioned nonlinearities in the modelling. The generated model is validated via a case of study with simulation results. This research is paramount because it introduces a more accurate (the actuator dynamics, a complex nonlinear subsystem) model that could be applied to one-half vehicle suspension control purposes. Suspension systems are extremely important for passenger comfort and stability in ground vehicles.

1. Introduction

Vehicle suspension systems have the objective of absorbing road disturbances, while keeping the tires in contact with the road surface [1–3]. At the same time it improves passenger comfort and vehicle stability in a certain level. The traditional, commercial oriented approach is the passive suspension, which is designed for comfort or stability purposes, due to its constant damping force value, and trade-off relation between comfort and stability. Since the 1960s, there have been technological advances in fabrication and control of special materials, referred to as rheological fluids [4]. Because these materials are able to change from viscous to semisolid in milliseconds, they have been applied to build new types of dampers. Afterward, generations of economically viable vehicle suspensions that modify their damping force in real-time became available. They are commonly known intelligent suspensions [5].

As part of intelligent semiactive suspensions and to the best of authors' knowledge, electrorheological (ER) and magnetorheological dampers are probably the most applied approaches, from which the latter has been the most explored option due to its low power consumption and safeness [6, 7]. By installing an MR damper in the suspension system, ride comfort and vehicle stability can be considerably increased. However, system's complexity is augmented because of the highly nonlinear phenomena inherent in the damper's composition [8]. As a result, modelling and control strategies for semiactive suspensions are two principal areas where automotive investigation has been concentrated.

It is well known that one-quarter suspension models are restricted to vertical motion [5], whereas one-half vehicle suspension representations extend the analysis to pitch or roll dynamics [9]. Moreover, the 4-DOF suspension approach developed herein is the so-called bicycle or lateral model, that is, a simplified model that merges both front wheels into a

single front one, and does the same with the rear wheels. Lateral model includes vertical motion of the concentrated front and rear wheels, as well as vertical and pitch dynamics of the sprung mass. There is reported work related to a half vehicle through the so-called bicycle model [10, 11]. Publications include vertical and roll dynamics as reported in Sammier et al. [12] and more recently in Jeon et al. [13] and Yu et al. [14]. Novel reported work has handled one-half suspension models, where the Bouc-Wen model has been applied for the complete control system, but without considering actuator's dynamics for control law computation [15, 16].

There is a considerable amount of literature related to one-half suspension control that applies diverse modelling approaches. However, most of them avoid nonlinear model dynamics; for example, Yagiz et al. [17] reported a robust fuzzy sliding-mode controller for an active one-half bicycle suspension with very complete results in time and frequency domains, although an opportunity area is to include the actuator dynamics, as reported in Félix-Herrán et al. [18]. Moreover, Cao et al. [19] reported a fuzzy controller for a one-half semiactive suspension, whereas El Messoussi et al. [20] went further and developed the T-S fuzzy modelling [21] and control for the four-wheel vehicle model, but in both cases, MR damper dynamics was left aside and no performance criteria in frequency domain were included.

Recently, Hametner et al. [22] proposed an algorithm based on grey-box modelling approach. The strategy considers the systems' nonlinearities and a case of study based on a half vehicle suspension is presented. The work compared the real vehicle behaviour against the proposed model. Regarding T-S fuzzy modelling, Li et al. [23] presented a lateral suspension representation through T-S methodology, but nonlinearities were not considered in the model. Kasprzyk and Krauze [24] went further and reported a half-car model that includes MR damper's dynamics; however, no T-S approach was employed. The obtained model and the applied control law are both nonlinear. Thus, an opportunity area is detected, if the global model has linear subsystems, the well-known control theory can be implemented, and T-S strategy becomes an advantageous option as employed herein. From these recent outcomes and previous work, the objective of this research is to develop a model that includes actuator's nonlinear dynamics following the T-S fuzzy approach. This combination is the herein contribution (taking the work in Félix-Herrán et al. [25] as the baseline).

This paper is organized as follows. Section 2 presents the 4-DOF one-half passive vehicle model. Section 3 develops the semiactive T-S fuzzy model. Section 4 presents the case of study based on real suspension and MR damper data. Simulations support theoretical outcomes. The ending section concludes the research and includes further research directions.

2. One-Half Passive Suspension Model

Modelling and control in a one-half 4-DOF vehicle suspension can be accomplished including vertical and pitch dynamics or vertical and roll movements [2]. The well-known bicycle model with vertical and pitch dynamics [26, 27] is the most mentioned one-half vehicle approach [9], and it is the one considered herein (depicted in Figure 1).

In Figure 1, the front tires are represented by a single element m_{tf}, and the rear tires by m_{tr}. As a result, the system has the capacity to turn over a pitch angle θ (positive when it grows clockwise). This rotation occurs around an imaginary axis that is transversal to sprung mass m_s. For the present study, m_s is considered to be a bar of length $(a + b)$ with a moment of inertia I_y. Furthermore, the centre of mass is not exactly in the middle of the vehicle; thus distances a and b, as well as front m_{tf} and rear m_{tr} unsprung masses, could be different.

For passive suspensions, k_{sf} and k_{sr} denote the front and rear suspension springs' constants. Besides, c_{sf} and c_{sr} are the dampers' constants. Moreover, the front tire is represented by k_{tf}, whereas the rear one is symbolized by k_{tr}. Front and back tires' displacements are Z_{tf} and Z_{tr} (upward direction in considered positive). Besides, Figure 1 portrays small displacements Z_{sf} and Z_{sr} that have to be included in the vertical analysis. Furthermore, system disturbance inputs come from the road profile in the form of Z_{rf} and Z_{rr}.

From Figure 1, a set of mathematical relations is generated, as presented in (1) to (4). These equations allow to analyse the significant variables related to vertical and pitch dynamics for a 4-DOF one-half vehicle suspension with a passive damper. The model developed herein considers three practical assumptions (pitch angle θ is smaller than 5°, thus $\sin\theta = \theta$ and $\cos\theta = 1$; front and rear MR dampers have similar characteristics; and gravity force effect on the vehicle is inherent in the suspension deflection value, and thus it can be removed from the equations of motion).

Coming out of Figure 1, the following equations are obtained:

$$\begin{aligned} m_s\ddot{Z}_s = &-\left(k_{sf}+k_{sr}\right)Z_s-\left(c_{sf}+c_{sr}\right)\dot{Z}_s \\ &+\left(ak_{sf}-bk_{sr}\right)\theta+\left(ac_{sf}-bc_{sr}\right)\dot{\theta} \\ &+k_{sf}Z_{tf}+c_{sf}\dot{Z}_{tf}+k_{sr}Z_{tr}+c_{sr}\dot{Z}_{tr}, \end{aligned} \tag{1}$$

$$\begin{aligned} I_y\ddot{\theta} = &\left(ak_{sf}-bk_{sr}\right)Z_s+\left(ac_{sf}-bc_{sr}\right)\dot{Z}_s \\ &-\left(a^2k_{sf}+b^2k_{sr}\right)\theta-\left(a^2c_{sf}+b^2c_{sr}\right)\dot{\theta} \\ &-ak_{sf}Z_{tf}-ac_{sf}\dot{Z}_{tf}+bk_{sr}Z_{tr}+bc_{sr}\dot{Z}_{tr}, \end{aligned} \tag{2}$$

$$\begin{aligned} m_{tf}\ddot{Z}_{tf} = &\,k_{sf}Z_s+c_{sf}\dot{Z}_s-ak_{sf}\theta-ac_{sf}\dot{\theta} \\ &-\left(k_{sf}+k_{tf}\right)Z_{tf}-c_{sf}\dot{Z}_{tf}+k_{tf}Z_{rf}, \end{aligned} \tag{3}$$

$$\begin{aligned} m_{tr}\ddot{Z}_{tr} = &\,k_{sr}Z_s+c_{sr}\dot{Z}_s+bk_{sr}\theta+bc_{sr}\dot{\theta} \\ &-\left(k_{sr}+k_{tr}\right)Z_{tr}-c_{sr}\dot{Z}_{tr}+k_{tr}Z_{rr}, \end{aligned} \tag{4}$$

where (1) refers to the unsprung mass motion and (2) to pitch dynamics. Equations (3) and (4) encompass front and rear tires acceleration, respectively.

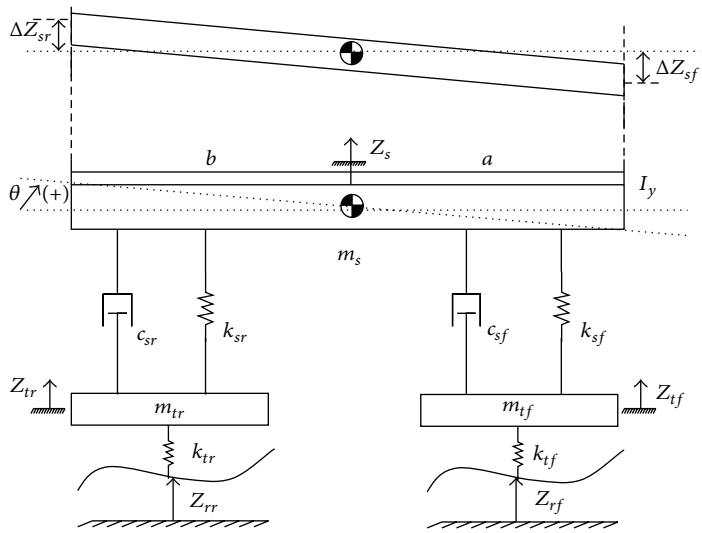

Figure 1: 4-DOF one-half passive suspension. The picture refers to the bicycle model.

3. Suspension with Two Magnetorheological Dampers

3.1. Modelling the Actuators' Nonlinearities. A passive suspension does not allow modifying the force delivered by the dampers. Hence, c_{sf} and c_{sr} are going to be replaced by a set of six elements (c_{0f}, k_{0f}, and hysteresis$_{\text{front}}$, c_{0f}, k_{0f}, and hysteresis$_{\text{rear}}$) that represents two MR dampers in order to vary suspension's damping factor. For the present study, front and rear dampers have similar characteristics, and they are modelled via Bouc-Wen approach [6], as reported in Félix-Herrán et al. [28]. The resulting suspension is depicted in Figure 2. This new representation includes the following dynamics:

$$\begin{aligned}
m_s\ddot{Z}_s &= -\left(k_{sf}+k_{0f}+k_{sr}+k_{0r}\right)Z_s-\left(c_{0f}+c_{0r}\right)\dot{Z}_s \\
&\quad+\left[a\left(k_{sf}+k_{0f}\right)-b\left(k_{sr}+k_{0r}\right)\right]\theta \\
&\quad+\left(ac_{0f}-bc_{0r}\right)\dot{\theta}+\left(k_{sf}+k_{0f}\right)Z_{tf} \\
&\quad+c_{0f}\dot{Z}_{tf}+\left(k_{sr}+k_{0r}\right)Z_{tr}+c_{0r}\dot{Z}_{tr} \\
&\quad-\alpha_f z_{\text{MR}f}-\alpha_r z_{\text{MR}r}, \\
I_y\ddot{\theta} &= \left[a\left(k_{sf}+k_{0f}\right)-b\left(k_{sr}+k_{0r}\right)\right]Z_s \\
&\quad+\left(ac_{0f}-bc_{0r}\right)\dot{Z}_s \\
&\quad-\left[\left(a^2\left(k_{sf}+k_{0f}\right)+b^2\left(k_{sr}+k_{0r}\right)\right)\right]\theta \\
&\quad-\left(a^2c_{0f}+b^2c_{0r}\right)\dot{\theta}-a\left(k_{sf}+k_{0f}\right)Z_{tf} \\
&\quad-ac_{0f}\dot{Z}_{tf}+b\left(k_{sr}+k_{0r}\right)Z_{tr}+bc_{0r}\dot{Z}_{tr} \\
&\quad+a\alpha_f z_{\text{MR}f}-b\alpha_f z_{\text{MR}r}, \\
m_{tf}\ddot{Z}_{tf} &= \left(k_{sf}+k_{0f}\right)Z_s+c_{0f}\dot{Z}_s-a\left(k_{sf}+k_{0f}\right)\theta \\
&\quad-ac_{0f}\dot{\theta}-\left(k_{sf}+k_{tf}+k_{0f}\right)Z_{tf}-c_{0f}\dot{Z}_{tf} \\
&\quad+\alpha_f z_{\text{MR}f}+k_{tf}Z_{rf}, \\
m_{tr}\ddot{Z}_{tr} &= \left(k_{sr}+k_{0r}\right)Z_s+c_{0r}\dot{Z}_s+b\left(k_{sr}+k_{0r}\right)\theta \\
&\quad+bc_{0r}\dot{\theta}-\left(k_{sr}+k_{tr}+k_{0r}\right)Z_{tr}-c_{0r}\dot{Z}_{tr} \\
&\quad+\alpha_r z_{\text{MR}r}+k_{tr}Z_{rr}.
\end{aligned} \tag{5}$$

According to Spencer Jr. et al. [6], and tailored for a 4-DOF one-half vehicle suspension, theoretical internal variables $z_{\text{MR}f}$ and $z_{\text{MR}r}$ are defined as follows:

$$\begin{aligned}
\dot{z}_{\text{MR}f} &= -\gamma_f\left|\dot{Z}_s-a\dot{\theta}-\dot{Z}_{tf}\right|z_{\text{MR}f}\left|z_{\text{MR}f}\right|^{n-1} \\
&\quad-\beta_f\left(\dot{Z}_s-a\dot{\theta}-\dot{Z}_{tf}\right)\left|z_{\text{MR}f}\right|^n \\
&\quad+A_f\left(\dot{Z}_s-a\dot{\theta}-\dot{Z}_{tf}\right), \\
\dot{z}_{\text{MR}r} &= -\gamma_r\left|\dot{Z}_s+b\dot{\theta}-\dot{Z}_{tr}\right|z_{\text{MR}r}\left|z_{\text{MR}r}\right|^{n-1} \\
&\quad-\beta_r\left(\dot{Z}_s+b\dot{\theta}-\dot{Z}_{tr}\right)\left|z_{\text{MR}r}\right|^n \\
&\quad+A_r\left(\dot{Z}_s+b\dot{\theta}-\dot{Z}_{tr}\right),
\end{aligned} \tag{6}$$

where $n = 2$, as explained by Wen [29]. Because this work employs A for other meanings, δ is adopted instead. Moreover, applied current into the actuator affects internal MR dampers' characteristics with the variation of c_{0f}, k_{0f}, α_f,

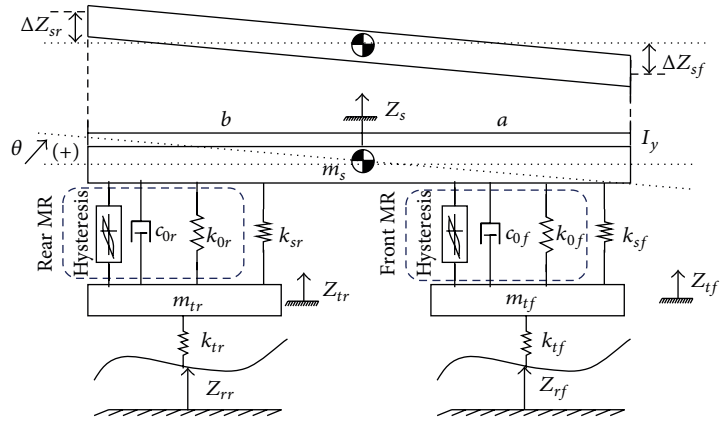

Figure 2: 4-DOF one-half semiactive suspension.

c_{0f}, k_{0f}, and α_r, as explained in Sireteanu et al. [30] and given below:

$$\begin{aligned} c_{0f} &= c_{0fa} + c_{0fb} i_f, \\ k_{0f} &= k_{0fa} + k_{0fb} i_f, \\ \alpha_f &= \alpha_{fa} + \alpha_{fb} i_f, \\ c_{0r} &= c_{0ra} + c_{0rb} i_r, \\ k_r &= k_{0ra} + k_{0rb} i_r, \\ \alpha_r &= \alpha_{ra} + \alpha_{rb} i_r, \end{aligned} \tag{7}$$

where i_f and i_r are the command inputs, that is, two different electrical current values to manipulate the front and rear MR dampers. The semiactive suspension is represented with (5) to (7).

3.2. Takagi-Sugeno Fuzzy Model. Following the approach in [28], a Takagi-Sugeno fuzzy model [31] needs to be obtained in order to synthesize a controller. The first step is to rearrange the equations of motion in such a way that nonlinearities can be clearly identified [25] and, if possible, to group them into one single nonlinearity. It is important to keep the number of nonlinearities as small as possible because the resulting T-S system is going to have $2^{(\#\text{nonlinearities})}$ linear subsystems [31]; therefore, present research considers the outcomes in Félix-Herrán et al. [25], in order to obtain a T-S model with fewer subsystems by considering Bouc-Wen approach instead of the Spencer model [6]. The latter is more accurate than the former, but more complex as well, and it generates a T-S model with more linear subsystems.

Due to suspension system's multiple input multiple output nature, it is appropriate to define a state-space model. Hence, the following state variables and inputs are designated.

$x_1 = Z_s$, $x_2 = \dot{Z}_s$, $x_3 = \theta$, $x_4 = \dot{\theta}$, $x_5 = Z_{tf}$, $x_6 = \dot{Z}_{tf}$, $x_7 = Z_{tr}$, $x_8 = \dot{Z}_{tr}$, $x_9 = z_{\text{MR}f}$, $x_{10} = z_{\text{MR}r}$, and $u_1 = i_f$, $u_2 = i_r$, $w_1 = Z_{rf}$, $w_2 = Z_{rr}$. Therefore, the entire system is reformulated to include state-space variables and nonlinearities Z_1 to Z_4:

$$\begin{aligned} \dot{x}_1 &= x_2, \\ m_s \dot{x}_2 &= -\left(k_{sf} + k_{0fa} + k_{sr} + k_{0ra}\right) x_1 \\ &\quad - \left(c_{0fa} + c_{0ra}\right) x_2 + (a-b)\left(k_{sf} + k_{0fa}\right) x_3 \\ &\quad + (a-b)\, c_{0fa} x_4 + \left(k_{sf} + k_{0fa}\right) x_5 + c_{0fa} x_6 \\ &\quad + \left(k_{sr} + k_{0ra}\right) x_7 + c_{0ra} x_8 - \alpha_f x_9 - \alpha_r x_{10} \\ &\quad + Z_1 u_1 + Z_2 u_2, \\ \dot{x}_3 &= x_4, \\ I_y \dot{x}_4 &= \left[a\left(k_{sf} + k_{0fa}\right) - b\left(k_{sr} + k_{0ra}\right)\right] x_1 \\ &\quad + \left(a c_{0fa} - b c_{0ra}\right) x_2 \\ &\quad - \left[a^2\left(k_{sf} + k_{0fa}\right) + b^2\left(k_{sr} + k_{0ra}\right)\right] x_3 \\ &\quad - \left(a^2 c_{0fa} + b^2 c_{0ra}\right) x_4 - a\left(k_{sf} + k_{0fa}\right) x_5 \\ &\quad - a c_{0fa} x_6 + b\left(k_{sr} + k_{0ra}\right) x_7 + b c_{0ra} x_8 \\ &\quad + a\alpha_{fa} x_9 - b\alpha_{ra} x_{10} - a Z_1 u_1 + b Z_2 u_2, \\ \dot{x}_5 &= x_6, \\ m_{tf} \dot{x}_6 &= \left(k_{sf} + k_{0fa}\right) x_1 + c_{0fa} x_2 - a\left(k_{sf} + k_{0fa}\right) x_3 \\ &\quad - a c_{0fa} x_4 - \left(k_{sf} + k_{0fa} + k_{tf}\right) x_5 - c_{0fa} x_6 \\ &\quad + \alpha_{fa} x_9 + k_{tf} w_1 - Z_1 u_1, \\ \dot{x}_7 &= x_8, \\ m_{tr} \dot{x}_8 &= \left(k_{sr} + k_{0ra}\right) x_1 + c_{0ra} x_2 + b\left(k_{sr} + k_{0ra}\right) x_3 \end{aligned}$$

$$
\begin{aligned}
&+ bc_{0ra}x_4 - \left(k_{sr} + k_{0ra} + k_{tr}\right)x_7 - c_{0ra}x_8 \\
&+ \alpha_{ra}x_{10} + k_{tr}w_2 - Z_2u_2, \\
\dot{x}_9 &= Z_3x_9 + \delta_f x_2 - a\delta_f x_4 - \delta_f x_6, \\
\dot{x}_{10} &= Z_4x_{10} + \delta_r x_2 + b\delta_r x_4 - \delta_r x_8.
\end{aligned} \tag{8}
$$

Z_1 to Z_4 are nonlinear terms defined as follows:

$$
\begin{aligned}
Z_1 &= -k_{0fb}x_1 - c_{0fb}x_2 + ak_{0fb}x_3 + ac_{0fb}x_4 + k_{0fb}x_5 \\
&\quad + c_{0fb}x_6 - \alpha_{fb}x_9, \\
Z_2 &= -k_{0rb}x_1 - c_{0rb}x_2 - bk_{0rb}x_3 - bc_{0rb}x_4 + k_{0rb}x_7 \\
&\quad + c_{0rb}x_8 - \alpha_{rb}x_{10}, \\
Z_3 &= -\left[\gamma_f \left|x_2 - ax_4 - x_6\right| \right. \\
&\quad \left. + \beta_f \left(x_2 - ax_4 - x_6\right) \operatorname{sgn}\left(x_9\right)\right] \left|x_9\right|, \\
Z_4 &= -\left[\gamma_r \left|x_2 + bx_4 - x_8\right| \right. \\
&\quad \left. + \beta_r \left(x_2 + bx_4 - x_8\right) \operatorname{sgn}\left(x_{10}\right)\right] \left|x_{10}\right|,
\end{aligned} \tag{9}
$$

where $\beta_f = \beta_r$, $\gamma_f = \gamma_r$, and $\delta_f = \delta_r$, considering that both MR dampers are identical. In addition, $\operatorname{sgn}(x_9)$ and $\operatorname{sgn}(x_{10})$ comply with

$$
\left|\zeta\right| = \zeta \operatorname{sgn}\left(\zeta\right), \tag{10}
$$

where $\operatorname{sgn}(\zeta)$ returns -1 if $\zeta < 0$, 0 if $\zeta = 0$, and $+1$ if $\zeta > 0$. In accordance with T-S modelling, Z_1 to Z_4 are going to be replaced by linear subsystems interconnected with fuzzy membership functions:

$$
\begin{aligned}
Z_1 &= M_1 Z_{1\max}u_1 + \left(1 - M_1\right) Z_{1\min}u_1, \\
Z_2 &= N_1 Z_{2\max}u_2 + \left(1 - N_1\right) Z_{2\min}u_2, \\
Z_3 &= P_1 Z_{3\max}x_9 + \left(1 - P_1\right) Z_{3\min}x_9, \\
Z_4 &= Q_1 Z_{4\max}x_{10} + \left(1 - Q_1\right) Z_{4\min}x_{10},
\end{aligned} \tag{11}
$$

where u_1 refers to the command input i_f and u_2 stands for the command input i_r from the front and rear MR dampers, respectively. Moreover, $Z_{1\max}$ is the upper bound of Z_1, whereas $Z_{1\min}$ is the lower bound of Z_1; that is, $Z_{1\max}$ and $Z_{1\min}$ are the maximum and minimum numerical values of Z_1. This same condition holds for Z_2, Z_3, and Z_4. Following the approach in Tanaka et al. [32]; M_1, M_2, N_1, N_2, P_1, P_2, Q_1, and Q_2 are fuzzy membership functions, and they are calculated from (11), as below:

$$
\begin{aligned}
M_1 &= \frac{\left[-k_{0fb}x_1 - c_{0fb}x_2 + ak_{0fb}x_3 + ac_{0fb}x_4 + k_{0fb}x_5 + c_{0fb}x_6 - \alpha_{fb}x_9\right] - Z_{1\min}}{Z_{1\max} - Z_{1\min}}, \\
M_2 &= 1 - M_1, \\
N_1 &= \frac{\left[-k_{0rb}x_1 - c_{0rb}x_2 - bk_{0rb}x_3 - bc_{0rb}x_4 + k_{0rb}x_7 + c_{0rb}x_8 - \alpha_{rb}x_{10}\right] - Z_{2\min}}{Z_{2\max} - Z_{2\min}}, \\
N_2 &= 1 - N_1, \\
P_1 &= \frac{\left[-\left[\gamma_f \left|x_2 - ax_4 - x_6\right| - \beta_f \left(x_2 - ax_4 - x_6\right) \operatorname{sgn}\left(x_9\right)\right] \left|x_9\right|\right] - Z_{3\min}}{Z_{3\max} - Z_{3\min}}, \\
P_2 &= 1 - P_1, \\
Q_1 &= \frac{\left[-\left[\gamma_r \left|x_2 + bx_4 - x_8\right| - \beta_r \left(x_2 + bx_4 - x_8\right) \operatorname{sgn}\left(x_{10}\right)\right] \left|x_{10}\right|\right] - Z_{4\min}}{Z_{4\max} - Z_{4\min}}, \\
Q_2 &= 1 - Q_1,
\end{aligned} \tag{12}
$$

where $M_1 + M_2 = 1$, $N_1 + N_2 = 1$, $P_1 + P_2 = 1$, and $Q_1 + Q_2 = 1$. If there are four nonlinearities, the system can be represented by $2^4 = 16$ linear subsystems interconnected through fuzzy membership functions defined in (12). Furthermore, each Z term is between a maximum (max) and a minimum (min) value. Each subsystem has the form of if. . .then rules, as fully explained in Takagi and Sugeno [21].

Likewise T-S fuzzy theory presented in Tanaka and Wang [31] and due to 4 nonlinearities, 16 fuzzy membership functions h_1 to h_{16} are defined. The total number of h

functions refers to all combinations with Z_s. The resulting 16 h equations are as follows:

$$\begin{aligned}
h_1 &= M_1N_1P_1Q_1,\\
h_2 &= M_1N_1P_1Q_2,\\
h_3 &= M_1N_1P_2Q_1,\\
h_4 &= M_1N_1P_2Q_2,\\
h_5 &= M_1N_2P_1Q_1,\\
h_6 &= M_1N_2P_1Q_2,\\
h_7 &= M_1N_2P_2Q_1,\\
h_8 &= M_1N_2P_2Q_2,\\
h_9 &= M_2N_1P_1Q_1,\\
h_{10} &= M_2N_1P_1Q_2,\\
h_{11} &= M_2N_1P_2Q_1,\\
h_{12} &= M_2N_1P_2Q_2,\\
h_{13} &= M_2N_2P_1Q_1,\\
h_{14} &= M_2N_2P_1Q_2,\\
h_{15} &= M_2N_2P_2Q_1,\\
h_{16} &= M_2N_2P_2Q_2.
\end{aligned} \tag{13}$$

As explained in Tanaka and Wang [31], (13) must comply with

$$0 \le h_i \le 1, \quad \sum_{i=1}^{n} h_i = 1. \tag{14}$$

Wrapping up nonlinearities, h functions, and membership functions, the one-half semiactive vehicle's suspension system can be expressed with a T-S fuzzy representation:

$$\dot{x}(t) = \sum_{i=1}^{16} h_i \left[A_i x(t) + B_i u(t)\right] + B_w w(t), \tag{15}$$

where

$$A_i = A + \Gamma_i \tag{16}$$

$$A = \begin{bmatrix}
0 & 1 & 0 & 0 & 0 & 0 & 0 & 0 & 0 & 0\\
A_{2,1} & A_{2,2} & A_{2,3} & A_{2,4} & A_{2,5} & A_{2,6} & A_{2,7} & A_{2,8} & A_{2,9} & A_{2,10}\\
0 & 0 & 0 & 1 & 0 & 0 & 0 & 0 & 0 & 0\\
A_{4,1} & A_{4,2} & A_{4,3} & A_{4,4} & A_{4,5} & A_{4,6} & A_{4,7} & A_{4,8} & A_{4,9} & A_{4,10}\\
0 & 0 & 0 & 0 & 0 & 1 & 0 & 0 & 0 & 0\\
A_{6,1} & A_{6,2} & A_{6,3} & A_{6,4} & A_{6,5} & A_{6,6} & 0 & 0 & A_{6,9} & 0\\
0 & 0 & 0 & 0 & 0 & 0 & 0 & 1 & 0 & 0\\
A_{8,1} & A_{8,2} & A_{8,3} & A_{8,4} & 0 & 0 & A_{8,7} & A_{8,8} & 0 & A_{8,10}\\
0 & \delta_f & 0 & -a\delta_f & 0 & -\delta_f & 0 & 0 & 0 & 0\\
0 & \delta_r & 0 & b\delta_r & 0 & -\delta_r & 0 & 0 & 0 & 0
\end{bmatrix}, \tag{17}$$

where elements in the second row of matrix A in (17) are

$$\begin{aligned}
A_{2,1} &= -\frac{\left(k_{0fa} + k_{sf} + k_{0ra} + k_{sr}\right)}{m_s},\\
A_{2,2} &= -\frac{\left(c_{0fa} + c_{0ra}\right)}{m_s},\\
A_{2,3} &= \frac{\left[a\left(k_{0fa} + k_{sf}\right) - b\left(k_{0ra} + k_{sr}\right)\right]}{m_s},\\
A_{2,4} &= \frac{\left(ac_{0fa} - bc_{0ra}\right)}{m_s},\\
A_{2,5} &= \frac{\left(k_{0fa} + k_{sf}\right)}{m_s},\\
A_{2,6} &= \frac{c_{0fa}}{m_s},\\
A_{2,7} &= \frac{\left(k_{0ra} + k_{sr}\right)}{m_s},\\
A_{2,8} &= \frac{c_{0ra}}{m_s},\\
A_{2,9} &= -\frac{\alpha_{fa}}{m_s},\\
A_{2,10} &= -\frac{\alpha_{ra}}{m_s}.
\end{aligned} \tag{18}$$

Moreover, elements in the fourth row are given below:

$$\begin{aligned}
A_{4,1} &= \frac{\left[a\left(k_{0fa} + k_{sf}\right) - b\left(k_{0ra} + k_{sr}\right)\right]}{I_y},\\
A_{4,2} &= \frac{\left(ac_{0fa} - bc_{0ra}\right)}{I_y},\\
A_{4,3} &= -\frac{\left[a^2\left(k_{0fa} + k_{sf}\right) + b^2\left(k_{0ra} + k_{sr}\right)\right]}{I_y},\\
A_{4,4} &= -\frac{\left(a^2c_{0fa} + b^2c_{0ra}\right)}{I_y},\\
A_{4,5} &= -\frac{a\left(k_{0fa} + k_{sf}\right)}{I_y},\\
A_{4,6} &= -\frac{ac_{0fa}}{I_y},\\
A_{4,7} &= \frac{b\left(k_{0ra} + k_{sr}\right)}{I_y},
\end{aligned}$$

$$A_{4,8} = \frac{bc_{0ra}}{I_y},$$
$$A_{4,9} = \frac{a\alpha_{fa}}{I_y},$$
$$A_{4,10} = -\frac{b\alpha_{fb}}{I_y}. \tag{19}$$

Furthermore, the elements in the sixth row of (17) are

$$A_{6,1} = \frac{\left(k_{0fa} + k_{sf}\right)}{m_{tf}},$$
$$A_{6,2} = \frac{c_{0fa}}{m_{tf}},$$
$$A_{6,3} = -\frac{a\left(k_{0fa} + k_{sf}\right)}{m_{tf}},$$
$$A_{6,4} = -\frac{ac_{0fa}}{m_{tf}},$$
$$A_{6,5} = -\frac{\left(k_{0fa} + k_{sf} + k_{tf}\right)}{m_{tf}},$$
$$A_{6,6} = -\frac{c_{0fa}}{m_{tf}},$$
$$A_{6,9} = \frac{\alpha_{fa}}{m_{tf}}. \tag{20}$$

Finally, the elements of the eighth row are listed:

$$A_{8,1} = \frac{\left(k_{0ra} + k_{sr}\right)}{m_{tr}},$$
$$A_{8,2} = \frac{c_{0ra}}{m_{tr}},$$
$$A_{8,3} = \frac{b\left(k_{0ra} + k_{sr}\right)}{m_{tr}},$$
$$A_{8,4} = \frac{bc_{0ra}}{m_{tr}},$$
$$A_{8,7} = -\frac{\left(k_{0ra} + k_{sr} + k_{tr}\right)}{m_{tr}},$$
$$A_{8,8} = -\frac{c_{0ra}}{m_{tr}},$$
$$A_{8,10} = \frac{\alpha_{ra}}{m_{tr}}. \tag{21}$$

In (17), matrix A is constant, whereas the variable part of A_i is given by Γ_i with

$$\Gamma_{13} = \Gamma_9 = \Gamma_5 = \Gamma_1,$$
$$\Gamma_{14} = \Gamma_{10} = \Gamma_6 = \Gamma_2,$$
$$\Gamma_{15} = \Gamma_{11} = \Gamma_7 = \Gamma_3,$$
$$\Gamma_{16} = \Gamma_{12} = \Gamma_8 = \Gamma_4, \tag{22}$$

where Γ_1 to Γ_4 are defined as four augmented matrices, as follows:

$$\Gamma_1 = \left(0_{10,8} \mid \begin{bmatrix} 0 & 0 & 0 & 0 & 0 & 0 & 0 & 0 & Z_{3\max} & 0 \\ 0 & 0 & 0 & 0 & 0 & 0 & 0 & 0 & 0 & Z_{4\max} \end{bmatrix}^T \right),$$
$$\Gamma_2 = \left(0_{10,8} \mid \begin{bmatrix} 0 & 0 & 0 & 0 & 0 & 0 & 0 & 0 & Z_{3\max} & 0 \\ 0 & 0 & 0 & 0 & 0 & 0 & 0 & 0 & 0 & Z_{4\min} \end{bmatrix}^T \right),$$
$$\Gamma_3 = \left(0_{10,8} \mid \begin{bmatrix} 0 & 0 & 0 & 0 & 0 & 0 & 0 & 0 & Z_{3\min} & 0 \\ 0 & 0 & 0 & 0 & 0 & 0 & 0 & 0 & 0 & Z_{4\max} \end{bmatrix}^T \right),$$
$$\Gamma_4 = \left(0_{10,8} \mid \begin{bmatrix} 0 & 0 & 0 & 0 & 0 & 0 & 0 & 0 & Z_{3\min} & 0 \\ 0 & 0 & 0 & 0 & 0 & 0 & 0 & 0 & 0 & Z_{4\min} \end{bmatrix}^T \right). \tag{23}$$

In addition, vectors B_i comply with the following conditions:

$$B_4 = B_3 = B_2 = B_1,$$
$$B_8 = B_7 = B_6 = B_5,$$
$$B_{12} = B_{11} = B_{10} = B_9,$$
$$B_{16} = B_{15} = B_{14} = B_{13}, \tag{24}$$

where B_1, B_5, B_9, and B_{13} are described as follows:

$$B_1 = \begin{bmatrix} 0 & \frac{z_{1\max}}{m_s} & 0 & -\frac{az_{1\max}}{I_y} & 0 & -\frac{z_{1\max}}{m_{tf}} & 0 & 0 & 0 & 0 \\ 0 & \frac{z_{2\max}}{m_s} & 0 & \frac{bz_{2\max}}{I_y} & 0 & 0 & 0 & -\frac{z_{2\max}}{m_{tr}} & 0 & 0 \end{bmatrix}^T,$$

$$B_5 = \begin{bmatrix} 0 & \frac{z_{1\max}}{m_s} & 0 & -\frac{az_{1\max}}{I_y} & 0 & -\frac{z_{1\max}}{m_{tf}} & 0 & 0 & 0 & 0 \\ 0 & \frac{z_{2\min}}{m_s} & 0 & \frac{bz_{2\min}}{I_y} & 0 & 0 & 0 & -\frac{z_{2\min}}{m_{tr}} & 0 & 0 \end{bmatrix}^T,$$

$$B_9 = \begin{bmatrix} 0 & \frac{z_{1\min}}{m_s} & 0 & -\frac{az_{1\min}}{I_y} & 0 & -\frac{z_{1\min}}{m_{tf}} & 0 & 0 & 0 & 0 \\ 0 & \frac{z_{2\max}}{m_s} & 0 & \frac{bz_{2\max}}{I_y} & 0 & 0 & 0 & -\frac{z_{2\max}}{m_{tr}} & 0 & 0 \end{bmatrix}^T, \quad (25)$$

$$B_{13} = \begin{bmatrix} 0 & \frac{z_{1\min}}{m_s} & 0 & -\frac{az_{1\min}}{I_y} & 0 & -\frac{z_{1\min}}{m_{tf}} & 0 & 0 & 0 & 0 \\ 0 & \frac{z_{2\min}}{m_s} & 0 & \frac{bz_{2\min}}{I_y} & 0 & 0 & 0 & -\frac{z_{2\min}}{m_{tr}} & 0 & 0 \end{bmatrix}^T.$$

Furthermore, disturbance vector B_w, which is common to all subsystems, is defined as

$$B_w = \begin{bmatrix} 0 & 0 & 0 & 0 & 0 & \frac{k_{tf}}{m_{tf}} & 0 & 0 & 0 & 0 \\ 0 & 0 & 0 & 0 & 0 & 0 & 0 & \frac{k_{tr}}{m_{tr}} & 0 & 0 \end{bmatrix}^T. \quad (26)$$

Considering the set of state variables at the beginning of this section, the state vector associated to (15) is $[Z_s \ \dot{Z}_s \ \theta \ \dot{\theta} \ Z_{tf} \ \dot{Z}_{tf} \ Z_{tr} \ \dot{Z}_{tr} \ z_{\mathrm{MR}f} \ z_{\mathrm{MR}r}]^T$, albeit the command input vector is $[i_f \ i_r]^T$, and disturbance input vector is $[Z_{rf} \ Z_{rr}]^T$.

Differential equations and T-S fuzzy models must have a similar behaviour. In next section, a numerical example is applied to compare the models.

4. Case of Study

Simulation results based on realistic data support the theoretical work in Section 3. The one-half vehicle suspension parameters are in Table 1.

MR damper numerical data are the same ones employed for the one-quarter case in Félix-Herrán et al. [28], and $\beta = 1.0 \times 10^6\ \mathrm{m}^{-2}$, $\gamma = 1.2 \times 10^6\ \mathrm{m}^{-2}$, and $\delta = 15$ are taken from a real MR damper characterization in Sireteanu et al. [30]. It is worthwhile to mention that real MR dampers do not respond instantaneously to current changes [6]. Herein simulations consider dampers' transient time $\eta = 190\ \mathrm{s}^{-1}$, as noticed in Sireteanu et al. [30].

Table 1: One-half vehicle suspension parameters for simulation work.

Parameter	Value
m_s	800 kg
I_y	1,400 kg/m^2
a	1.38 m
b	1.36 m
$m_{tf} = m_{tr}$	40 kg
$k_{sf} = k_{sr}$	20,000 N/m
$k_{tf} = k_{tr}$	210,000 N/m
$c_{sf} = c_{rf}$	1,000 Ns/m

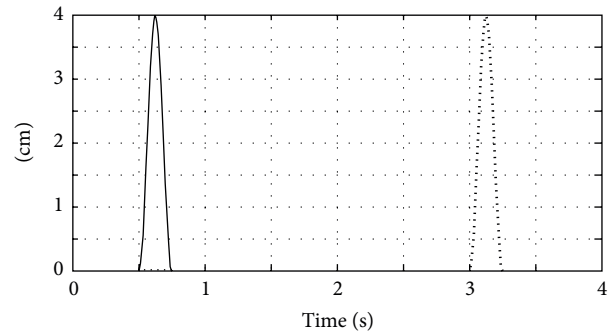

Figure 3: Road bump-like signal.

Keeping in mind that more linear subsystems generate a more complex T-S fuzzy model, Félix-Herrán et al. [28] presented a simplified approximation for $c_{0f}, k_{0f}, \alpha_f, c_{0f}, k_{0f}$, and α_r, as functions of current (i) into the MR dampers. This approach is employed as follows:

$$\begin{aligned} k_{0f} &= k_{0r} = 604.1 - 256.8i \ (\mathrm{N/m}), \\ c_{0f} &= c_{0r} = 516.6 + 144.9i \ (\mathrm{Ns/m}), \\ \alpha_f &= \alpha_r = 53290 + 29013i \ (\mathrm{N/m}), \end{aligned} \quad (27)$$

where i stands for either i_f or i_r, which are within the range [0.18–1.75] A to work in the most linear range of c_0, k_0, and α. Z_1 to Z_4 are defined as in (9) and their ranges (maximum and minimum values) are closely related to the gains computation [28].

There is a practical aspect to be considered before calculating the controller gains by reducing system's matrices ill-conditioning. Bouc-Wen parameters β, γ, and δ can be modified in such a way that MR dampers' response maintains almost the same behaviour; hence, a heuristically modification is applied in this work with the following values: $\beta = \gamma = 1.0 \times 10^5\ \mathrm{m}^{-2}$, and $\delta = 1.37$. With this action, a gap between the nonlinear differential equations and T-S models is introduced; however, accuracy is kept within an acceptable error range. Furthermore, present research considers that both dampers (front and rear) have the same characteristics.

For the T-S fuzzy modelling, based on (11), and considering that disturbance inputs from the ground are limited to a sinusoidal signal within the range [0–5] Hz and a road bump

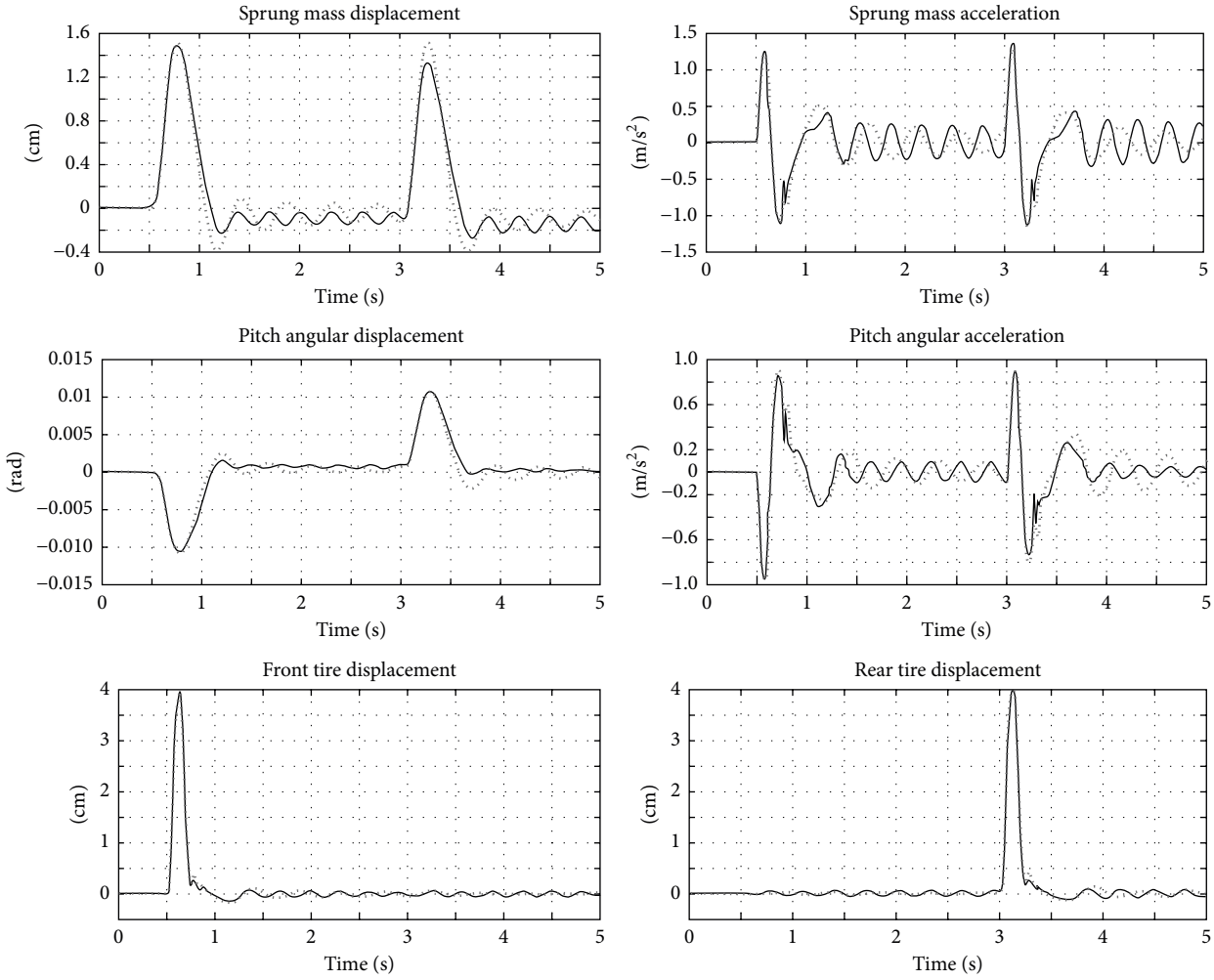

Figure 4: Road bump test. Both currents to MR dampers are set to a fixed value of 0.80 A.

of 0.04 m high, $Z_{1\max} = 162$, $Z_{1\min} = -190$, $Z_{2\max} = 161$, $Z_{2\min} = -195$, $Z_{3\max} = -2.6$, $Z_{3\min} = -407.20$, $Z_{4\max} = -2.65$, and $Z_{4\min} = -409$. Therefore, M_1, M_2, N_1, N_2, P_1, P_2, Q_1, and Q_1 are defined as in (12). Moreover, 16 fuzzy membership functions, h_1 to h_{16}, are defined as in (13) and they comply with (14). As a result, the T-S system in (15) was obtained, and the model has to be tested regarding stability in closed-loop.

T-S fuzzy model validation consists in a series of time response comparisons between T-S differential equations models. The set of variables involved in the suspension system are those proposed (state variables) in the beginning of Section 3.2. Herein tests apply two different road disturbances: a road bump and a sinusoidal signal. Road bump-like signals are commonly applied to review time domain suspensions' response, whereas sinusoidal ones are often employed to analyse suspensions' frequency domain response [12, 30].

In Figure 3, there is a road bump disturbance input of 0.04 m high. From the bicycle model perspective, the road bump affects the front wheel at 0.5 s in the form of Z_{rf}, and the same pulse turns into Z_{rr}, at 3.0 s, acting on the rear wheel. This input is represented by (28), as reported in Wu et al. [27]:

$$\begin{aligned} Z_{rf}(t) &= 0.04\,(1-\cos 8\pi t)\ (\mathrm{m}), \\ &\qquad \text{in the range of } 0.50 \le t \le 0.75\ (\mathrm{s}) \\ Z_{rr}(t) &= 0.04\,(1-\cos 8\pi t)\ (\mathrm{m}), \\ &\qquad \text{in the range of } 3.00 \le t \le 3.25\ (\mathrm{s}). \end{aligned} \tag{28}$$

Simulations compare the nonlinear differential suspension against its T-S fuzzy counterpart. For each case, the following variables are sketched: chassis displacement, chassis vertical acceleration, pitch angle displacement, pitch angle acceleration, front tire displacement, and rear tire displacement. Simulation time is set to 5.0 s. Figures 4 and 5 portray the comparisons for the road bump signal, whereas Figure 6 exposes the sinusoidal input test. In Figures 4 to 6, the light grey dotted line represents the T-S model response in (15),

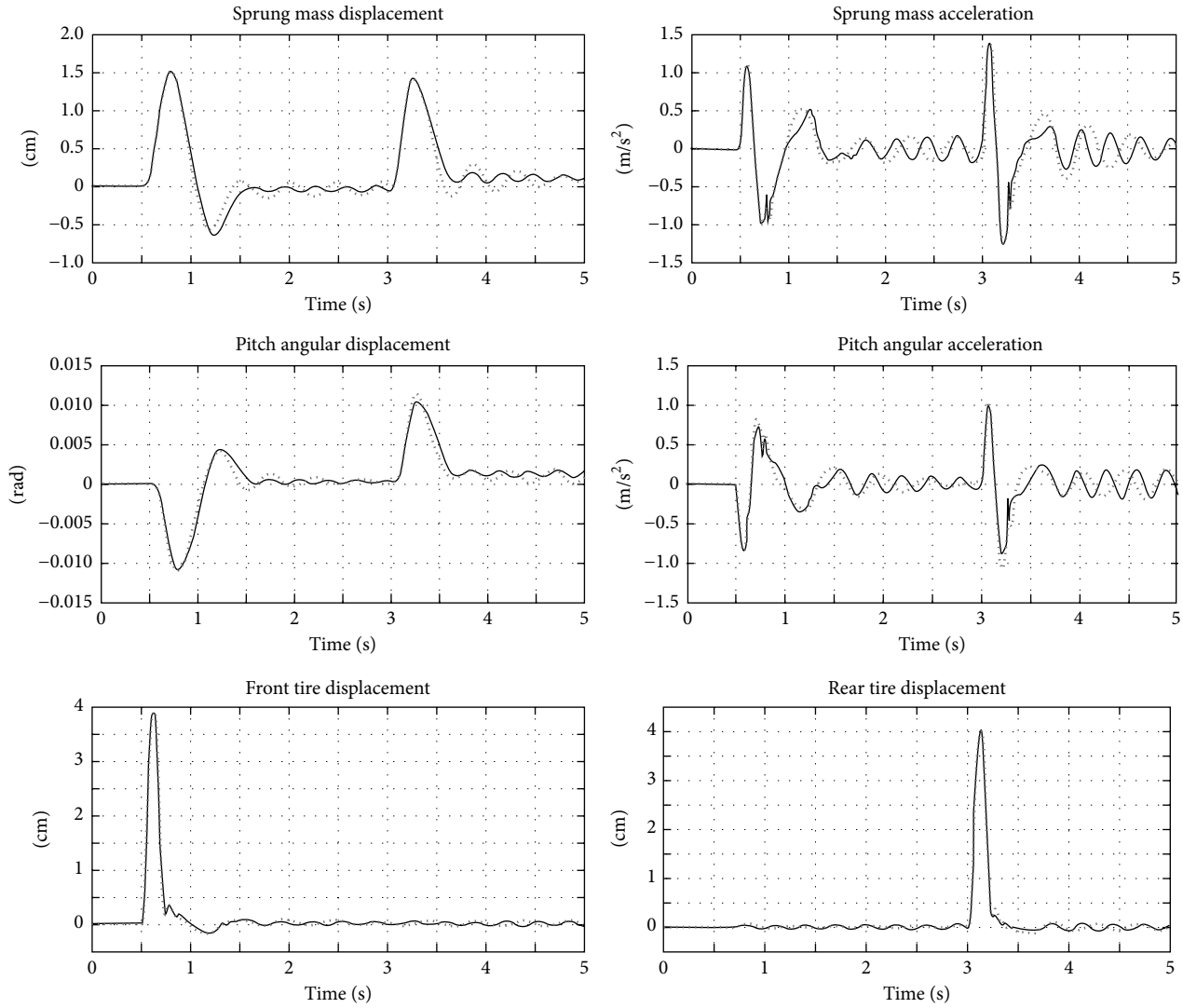

Figure 5: Road bump test. The front MR damper receives 0.20 A, and the rear is fed with 1.75 A.

and the black solid line indicates the nonlinear model in (5) to (7).

A second test is run for a sinusoidal disturbance of proper characteristics [12]. The herein sine input is modelled by

$$Z_{rf}(t) = 0.015 \sin(2\pi t)\ (\mathrm{m}),$$
$$Z_{rr}(t) = 0.015 \sin(2\pi t + 1.033)\ (\mathrm{m}). \tag{29}$$

Results in Figures 4 to 6 provide evidence about the likeness between differential equations and T-S fuzzy models. Even though some response differences are exposed, both representations have, in general, the same dynamics, and this is enough to apply T-S modelling, as the baseline for further control synthesis.

5. Conclusions and Future Work

The T-S fuzzy modelling approach contributes to develop a theoretical suspension representation that includes the actuator dynamics. The proposed novel keeps the main behaviour of the original differential equations suspension model, with the advantage of being represented in a suitable formulation that allows applying the well-known linear control theory. A case of study with simulations results supports the proposed outcomes.

The work herein goes beyond the outcomes in [25]. Moreover, it has the potential to be useful for [13–16], where no actuator dynamics are considered. In addition, the outcomes achieved in the present research provide a viable alternative to the recent in [22–24], by means of a 4-DOF one-half vehicle suspension with two magnetorheological nonlinear dampers. Control possibilities include fuzzy, H_∞, and H_2 strategies, among others.

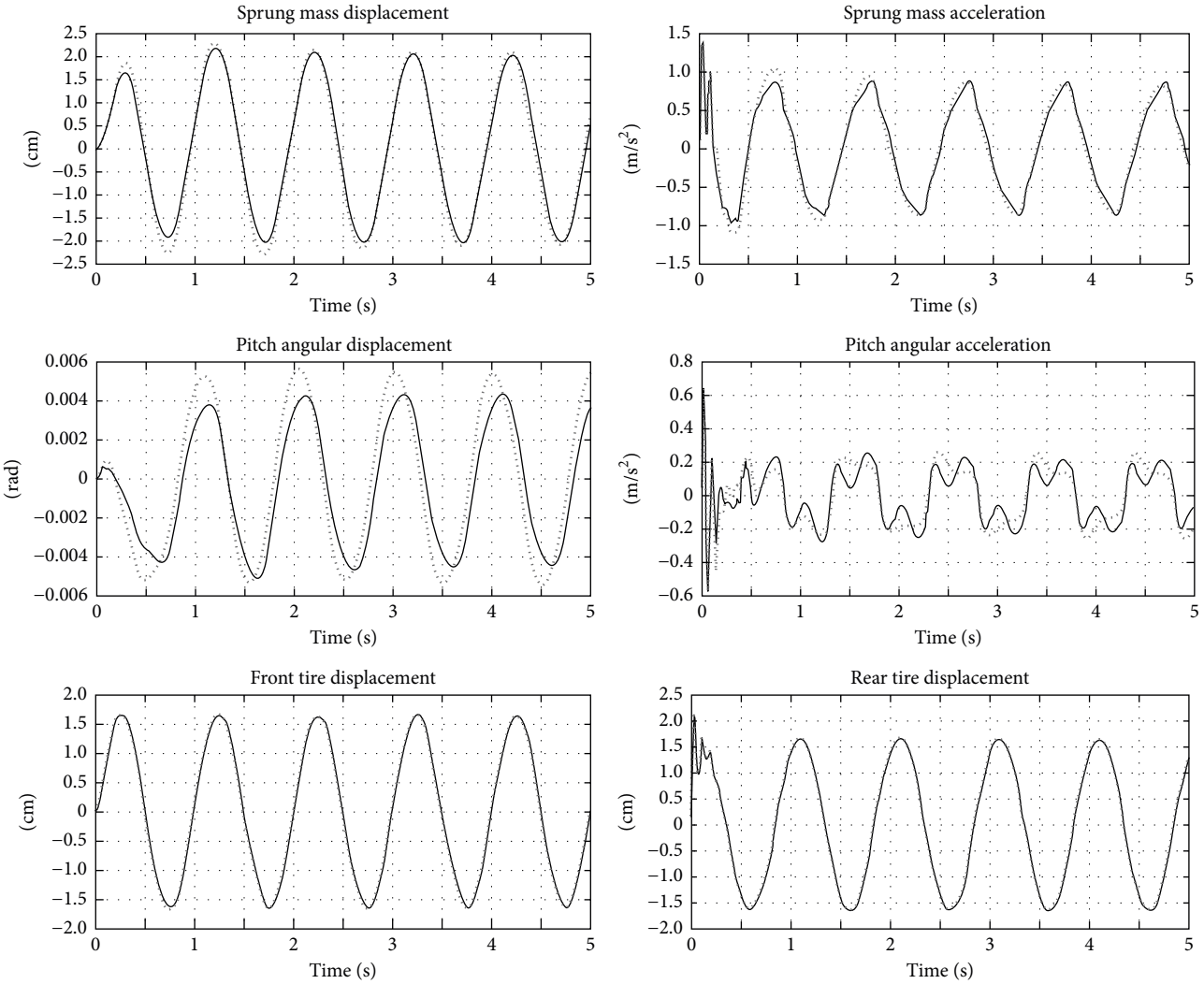

Figure 6: Sinusoidal disturbance. The front damper is connected to 1.70 A, and the rear one to 0.30 A.

At this moment, the opportunity area is T-S fuzzy model accuracy. Exhaustive work is required to identify the exact T-S nonlinearities boundaries, according to disturbances and control signals. Present work required a large set of tests considering all scenarios. Another limitation is that each nonlinear term is divided into two subsystems; hence, it is important to be assertive when defining nonlinearities because T-S formulation can grow in complexity.

Finally, this research is outstanding because it aims to obtain vehicle suspensions that meet comfort and stability standards (two aspects very valuable in automotive industry). This effort provides another step of the complete global chassis control in ground vehicles.

Conflict of Interests

The authors declare that there is no conflict of interests regarding the publication of this paper.

Acknowledgments

Authors are grateful to the Consejo Nacional de Ciencia y Tecnología (CONACYT), México, and Tecnológico de Monterrey, through the Robotics focus group for supporting and funding this research.

References

[1] T. Gillespie, *Fundamentals of Vehicle Dynamics*, SAE International, Warrendale, Pa, USA, 1992.

[2] W. Milliken and D. Milliken, *Race Car Vehicle Dynamics*, SAE International, Troy, Mich, USA, 1995.

[3] J. Y. Wong, *Theory of Ground Vehicles*, John Wiley and Sons, New York, NY, USA, 2001.

[4] D. J. Jeffrey and A. Acrivos, "The rheological properties of suspensions of rigid particles," *AIChE Journal*, vol. 22, no. 3, pp. 417–432, 1976.

[5] J. P. Pauwelussen and H. B. Pacejka, *Smart Vehicles*, Swets & Zeitlinger, London, UK, 1995.

[6] B. F. Spencer Jr., S. J. Dyke, M. K. Sain, and J. D. Carlson, "Phenomenological model for magnetorheological dampers," *Journal of Engineering Mechanics*, vol. 123, no. 3, pp. 230–238, 1997.

[7] R. Stanway, "The development of force actuators using ER and MR fluid technology," in *Proceedings of the IEE Colloquium on Actuator Technology: Current Practice and New Developments*, pp. 6/1–6/5, London, UK, May 1996.

[8] G. R. Worden and K. Tomlinson, *Nonlinearity in Structural Dynamics: Detection, Identification and Modeling*, IoP Publishing, London, UK, 2000.

[9] R. N. Jazar, *Vehicle Dynamics: Theory and Applications*, Springer, New York, NY, USA, 2008.

[10] A. G. Thompson and B. R. Davis, "Computation of the rms state variables and control forces in a half-car model with preview active suspension using spectral decomposition methods," *Journal of Sound and Vibration*, vol. 285, no. 3, pp. 571–583, 2005.

[11] M. Yu, X. M. Dong, S. B. Choi, and C. R. Liao, "Human simulated intelligent control of vehicle suspension system with MR dampers," *Journal of Sound and Vibration*, vol. 319, no. 3-5, pp. 753–767, 2009.

[12] D. Sammier, O. Sename, L. Dugard, and D. Sammier, "H_∞ control of active vehicle suspensions," in *Proceedings of the IEEE International Conference on Control Applications*, pp. 976–981, 2000.

[13] K. Jeon, H. Hwang, S. Choi, J. Kim, K. Jang, and K. Yi, "Development of an electric active rollcontrol (ARC) algorithm for a SUV," *International Journal of Automotive Technology*, vol. 13, no. 2, pp. 247–253, 2012.

[14] S. Yu, Z. Wu, F. Wang, and H. Chen, "Full-car active suspension based on H2/generalized H2 output feedback control," in *Proceedings of the IEEE International Conference on Control Applications (CCA '13)*, pp. 241–246, Hyderabad, India, August 2013.

[15] M. A. Eltantawie, "Decentralized neuro-fuzzy control for half car with semi-active suspension system," *International Journal of Automotive Technology*, vol. 13, no. 3, pp. 423–431, 2012.

[16] P. Krauze and J. Kasprzyk, "FxLMS algorithm with preview for vibration control of a half-car model with magnetorheological dampers," in *Proceedings of the IEEE/ASME International Conference on Advanced Intelligent Mechatronics*, pp. 518–523, 2014.

[17] N. Yagiz, Y. Hacioglu, and Y. Taskin, "Fuzzy sliding-mode control of active suspensions," *IEEE Transactions on Industrial Electronics*, vol. 55, no. 11, pp. 3883–3890, 2008.

[18] L. C. Félix-Herrán, J. D. J. Rodríguez-Ortiz, R. Soto, and R. Ramírez-Mendoza, "Modeling and control for a semi-active suspension with a magnetorheological damper including the actuator dynamics," in *Proceedings of the 5th Meeting of the Electronics, Robotics and Automotive Mechanics Conference (CERMA '08)*, pp. 338–343, October 2008.

[19] J. Cao, P. Li, and H. Liu, "An interval fuzzy controller for vehicle active suspension systems," *IEEE Transactions on Intelligent Transportation Systems*, vol. 11, no. 4, pp. 885–895, 2010.

[20] W. El Messoussi, O. Pagès, and A. El Hajjaji, "Four-wheel steering vehicle control using takagi-sugeno fuzzy models," in *Proceedings of the IEEE International Fuzzy Systems Conference*, pp. 1–6, July 2007.

[21] T. Takagi and M. Sugeno, "Fuzzy identification of systems and its applications to modeling and control," *IEEE Transactions on Systems, Man and Cybernetics*, vol. 15, no. 1, pp. 116–132, 1985.

[22] C. Hametner, J. Edelmann, S. Jakubek, and W. Mack, "An advanced algorithm for partitioning and parameter estimation in local model networks and its application to vehicle vertical dynamics," *Acta Mechanica*, vol. 223, no. 8, pp. 1693–1706, 2012.

[23] H. Li, J. Yu, C. Hilton, and H. Liu, "Adaptive sliding-mode control for nonlinear active suspension vehicle systems using T-S fuzzy approach," *IEEE Transactions on Industrial Electronics*, vol. 60, no. 8, pp. 3328–3338, 2013.

[24] J. Kasprzyk and P. Krauze, "Vibration control for a half-car model with adaptation of the magnetorheological damper model," in *Proceedings of the International Conference on Mode lling, Identification and Control*, pp. 243–248, 2014.

[25] L. Félix-Herrán, D. Mehdi, R. Soto, J. de J. Rodríguez-Ortiz, and R. Ramírez-Mendoza, "Control of a semi-active suspension with a magnetorheological damper modeled via Takagi-Sugeno," in *Proceedings of the 18th Mediterranean Conference on Control & Automation (MED '10)*, pp. 1265–1270, June 2010.

[26] R. Rajamani, *Vehicle Dynamics and Control*, Springer, New York, NY, USA, 2006.

[27] S.-J. Wu, C.-T. Wu, and T.-T. Lee, "Neural-network-based optimal fuzzy control design for half-car active suspension systems," in *Proceedings of the IEEE Intelligent Vehicles Symposium*, pp. 376–381, IEEE, June 2005.

[28] L. C. Félix-Herrán, D. Mehdi, J. D. J. Rodrguez-Ortiz, R. Soto, and R. Ramrez-Mendoza, "H_∞ control of a suspension with a magnetorheological damper," *International Journal of Control*, vol. 85, no. 8, pp. 1026–1038, 2012.

[29] Y.-K. Wen, "Method for random vibration of hysteretic systems," *Journal of the Engineering Mechanics Division*, vol. 102, no. 2, pp. 249–263, 1976.

[30] T. Sireteanu, D. Stancioiu, and C. W. Stammers, "Modelling of magnetorheological fluid dampers," *Proceedings of the Romanian Academy, Series A*, vol. 2, no. 3, pp. 27–31, 2001.

[31] K. Tanaka and H. Wang, *Fuzzy Control Systems Design and Analysis*, John Wiley & Sons, New York, NY, USA, 2001.

[32] K. Tanaka, T. Ikeda, and H. O. Wang, "Robust stabilization of a class of uncertain nonlinear systems via fuzzy control: quadratic stabilizability, H^∞ control theory, and linear matrix inequalities," *IEEE Transactions on Fuzzy Systems*, vol. 4, no. 1, pp. 1–13, 1996.

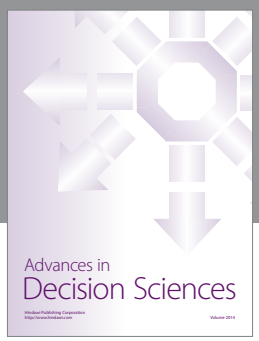

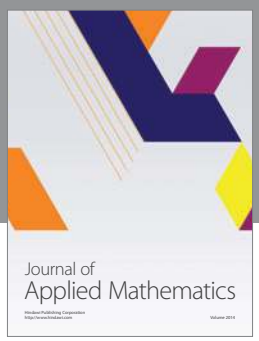

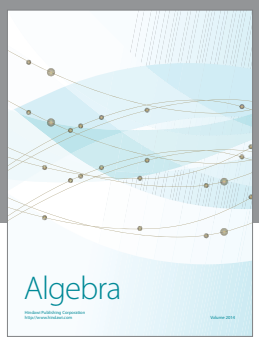

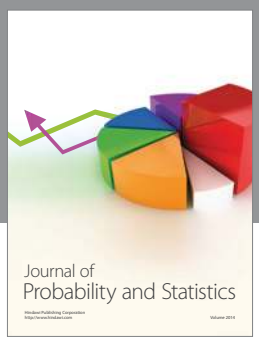

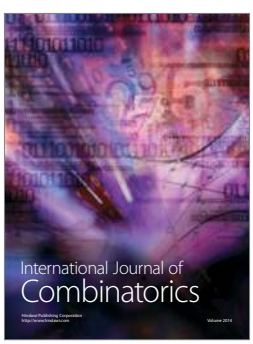

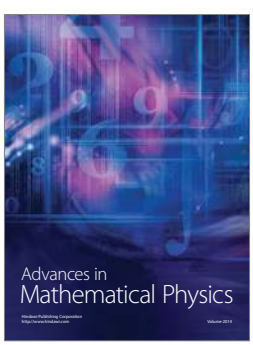

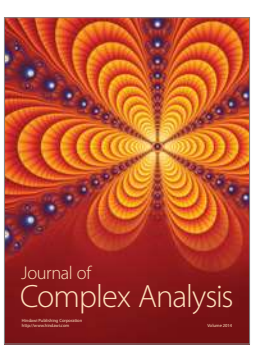

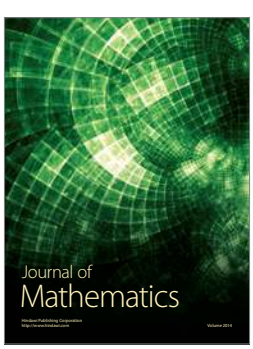

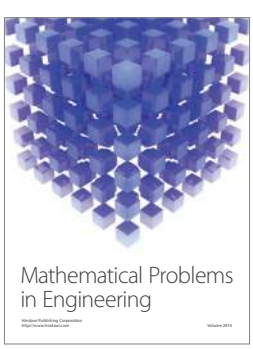

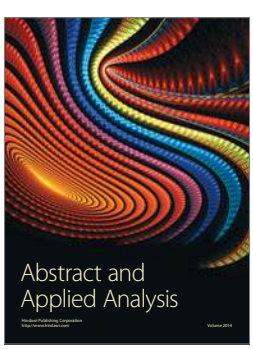

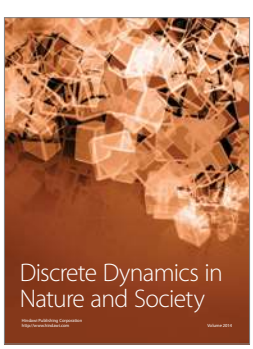

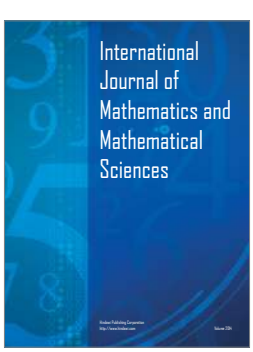

Hindawi
Submit your manuscripts at
http://www.hindawi.com